

See discussions, stats, and author profiles for this publication at: <https://www.researchgate.net/publication/259468065>

# Correlated Dynamical Crossovers of the Hydration Layer of a Single-Stranded DNA Oligomer

ARTICLE in THE JOURNAL OF PHYSICAL CHEMISTRY B · DECEMBER 2013

Impact Factor: 3.3 · DOI: 10.1021/jp408234k · Source: PubMed

---

CITATIONS

6

---

READS

47

2 AUTHORS, INCLUDING:



[Sanjoy Bandyopadhyay](#)

IIT Kharagpur

74 PUBLICATIONS 2,062 CITATIONS

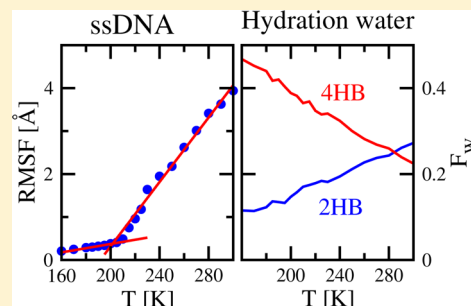
SEE PROFILE

# Correlated Dynamical Crossovers of the Hydration Layer of a Single-Stranded DNA Oligomer

Kaushik Chakraborty and Sanjoy Bandyopadhyay\*

Molecular Modeling Laboratory, Department of Chemistry, Indian Institute of Technology, Kharagpur 721302, India

**ABSTRACT:** Atomistic molecular dynamics (MD) simulations at different temperatures ranging from 160 to 300 K have been carried out to explore the correlated dynamical transitions of a single-stranded DNA (ss-DNA) oligomer with heterogeneous distribution of nucleobases, 5'-CGCGAATTCGCG-3', and that of its hydration water. The calculations reveal a distinct dynamical crossover of the DNA oligomer associated with abrupt changes of motions of its atoms at around 200–220 K. Importantly, it is found from calculated water diffusivities and relaxation times that the hydration water molecules also exhibit a crossover within 210–220 K. This indicates that the dynamical crossover of the DNA strand is coupled with that exhibited by its hydration water. In addition, another crossover point for the surface water molecules has been found around 180–185 K with the water layer exhibiting highly frozen dynamics. The rearrangement of hydrogen bond network that occurs due to population transition from two-coordinated to four-coordinated tetrahedrally arranged water molecules at the interface with lowering of temperature is found to be the microscopic origin of such correlated two-step dynamic crossovers of hydration water. Such modified hydrogen bonding results in transformation of hydration layer water structuring from high density to low density liquid under supercooled conditions.



## 1. INTRODUCTION

It is known that the activity of a biomolecule is uniquely correlated with its three-dimensional structure.<sup>1,2</sup> However, to perform its activity, it is essential for the biomolecule to exhibit certain critical conformational fluctuations. Molecular motions associated with the conformational fluctuations often occur over a wide range of time scales, between picoseconds to milliseconds or even longer. Under physiological conditions, the specific time scale associated with a particular motion often determines the reaction pathway and the rate associated with a biological process.

The governing forces behind the atomic motions in biomolecules originate from electrostatic, van der Waals, and hydrogen-bonding interactions. At room temperature, the energies associated with such forces are often close to the thermal energy, thereby making the biological matter soft. At low temperatures, biomolecules like proteins, DNA, etc., usually remain in harmonic modes trapped in specific conformations and act like hard materials without any activity.<sup>3</sup> With an increase in temperature, thermal motions of the biomolecule become anharmonic, with the atoms, instead of vibrating around equilibrium positions in harmonic modes, being able to jump between different conformational substates through large scale collective motions.<sup>4</sup> This eventually leads to diffusive motions of the molecule at relatively higher temperatures. Such “dynamical transitions” (often termed as “glass-like” transitions) from harmonic to anharmonic or diffusive mode are generally found to occur at around 200–240 K for biomolecules like proteins, DNA, RNA, etc., as evident from different experimental<sup>15–14</sup> and simulation studies.<sup>15–19</sup> The fact that dehydrated proteins do not exhibit such transitions showed

that water plays an important role in this process.<sup>20,21</sup> It is in fact known that an optimum water content is essential for the onset of critical conformational motions of a biomolecule to express its activity.<sup>22,23</sup> Simulation studies have shown that the glassy transitions of hydrated proteins are associated with restructuring of interfacial hydrogen bonds and their slow relaxations.<sup>15,24,25</sup> The importance of hydrogen bonds in controlling the dynamic transitions of biomolecules has also been confirmed from experiments.<sup>26</sup> The transition temperature is also found to be highly sensitive to the viscosity of the solvent.<sup>27,28</sup> Interestingly, it is found that water molecules hydrating the surface of a protein also exhibit some kind of transition within the temperature range similar to that observed for the protein.<sup>29–32</sup> This leads to a crucial question whether the dynamical crossovers observed for biomolecules are coupled with that of the surrounding solvent.

Although the dynamical transitions of proteins in aqueous solutions have been widely studied, only limited attempts are made to probe the existence of such transitions for DNA molecules. In an early work, Norberg and Nilsson<sup>33</sup> characterized the dynamical transitions of DNA from molecular dynamics (MD) simulations. Later, Stanley and co-workers<sup>34</sup> showed that the liquid–liquid transition in water induces a dynamical crossover of DNA. Low temperature dynamical crossovers of water in DNA grooves have also been identified recently by Bagchi and co-workers.<sup>31</sup> It may be noted that most of the works reported on DNA are carried out with their duplex

Received: August 17, 2013

Revised: December 26, 2013

Published: December 26, 2013

forms. However, to the best of our knowledge, no such attempt has been made so far to explore whether single-stranded DNA (ss-DNA) molecules in aqueous media exhibit similar dynamical transitions at low temperatures. This is primarily due to the difficulty in characterizing the structurally disordered ss-DNAs with high degree of conformational flexibilities.<sup>35</sup>

In this work, we attempt to explore for the first time the evidence for dynamic transition of an ss-DNA oligomer and its coupling, if any, with the dynamic relaxations of its hydration water. This is an important problem as ss-DNAs play crucial roles as intermediates in different biological processes, such as DNA replication, transcription, recombination, repair, etc.<sup>36</sup> In absence of the complementary strand, the nucleobases of an ss-DNA oligomer besides its charged backbone are expected to be more exposed to water and interact strongly with it.<sup>37</sup> Therefore, the conformational motions of ss-DNA should be coupled with the structural arrangement and dynamics of surrounding water molecules in an aqueous environment. In fact, several experimental studies have shown presence of water molecules bound to the nucleobases in site specific manners resulting in shortening of ss-DNA chains in aqueous media.<sup>38,39</sup> As a result, ss-DNAs are found neither in completely extended conformations or in significantly compact forms.<sup>35,38</sup> Recently, Miyasaka and co-workers<sup>40</sup> studied the long-time conformational relaxations of ss-DNA molecules in aqueous environment using time-resolved fluorescence spectroscopy. Three main conformations of the DNA oligomers were found with two interconversion time constants within several hundreds of nanoseconds to tens of microseconds. From theoretical analysis, Buhot and Halperin<sup>41</sup> showed that ss-DNA oligomers exhibit stacked domains in between melted random coil conformations. Further, it is shown from MD simulations that the structure and dynamics of nucleic acid strands depend on the nature of the backbone and formation of hydrogen bonds with water.<sup>42</sup>

In this article, we have carried out atomistic MD simulations of an aqueous solution of the ss-DNA oligomer with heterogeneous base sequences, 5'-CGCGAATTCGCG-3' at different temperatures ranging from 160 to 300 K. Attempts have been made to probe the microscopic origin of the coupled dynamical transitions of the DNA strand and its hydration water. The rest of the article is organized as follows. In section 2, we provide a brief description of the setup of the systems and the simulation methods employed. The results obtained from our investigations are presented and discussed in the following section (section 3). The important findings from our study and the conclusions reached therefrom are highlighted in section 4.

## 2. SIMULATION DETAILS

We have used the NAMD<sup>43</sup> code to carry out the MD simulations. The all-atom CHARMM force field for nucleic acids<sup>44,45</sup> were employed to describe the interactions between the DNA atoms, while the TIP3P model<sup>46</sup> which is consistent with the chosen nucleic acid force field, was used for water.

As described in our earlier work,<sup>37</sup> the initial coordinates of the DNA strand were obtained by unzipping the chain A of the Dickerson–Drew dodecamer (DDD) from the protein data bank (PDB ID: 436D).<sup>47</sup> Addition of hydrogen atoms and capping of the two end residues by replacing the phosphate groups with hydroxyl groups were done next. The DNA oligomer was then immersed in a cubic cell of edge length 60 Å containing equilibrated water molecules. The unfavorable contacts between the DNA and the solvent were avoided

during the insertion process by carefully removing those water molecules that were present within 2 Å from the DNA chain. The overall charge of the system was neutralized by adding 11 Na<sup>+</sup> ions. Finally, the system contained the ss-DNA molecule (379 atoms) in a cubic cell containing 7632 water molecules and 11 Na<sup>+</sup> ions.

To avoid any initial stress, the system was first minimized using the conjugate gradient energy minimization method as implemented in the NAMD code.<sup>43</sup> This minimized DNA–water system was used to carry out our study at 20 different temperatures between 160 to 300 K (with gaps of 5 K for the runs between 180 to 230 and 10 K for the rest). The temperature set for each simulation was gradually achieved within a short MD run of about 100 ps under isothermal–isobaric ensemble (NPT) conditions at a constant pressure ( $P = 1$  atm). This was followed by an NPT run with isotropic cell volume fluctuations for about 30 ns at each of the temperatures. Therefore, the total length of the simulations carried out was over 600 ns duration. While the Langevin dynamics method with a friction constant of 1 ps<sup>−1</sup> was used to control the system temperatures, the pressures were controlled by the Nosé–Hoover Langevin piston method.<sup>48</sup> The edge lengths ( $l_a$ ) of the simulation cells at the end of the NPT runs at different temperatures are listed in Table 1. The simulations were carried

**Table 1. Edge Lengths ( $l_a$ ) of the Cubic Simulations Cells As Obtained from the NPT Runs at Different Temperatures (T)**

temperature (K)	$l_a$ (Å)	temperature (K)	$l_a$ (Å)
160	59.92	220	60.01
170	59.86	225	60.22
180	59.84	230	60.23
185	59.86	240	60.30
190	59.93	250	60.40
195	59.91	260	60.52
200	59.94	270	60.64
205	59.94	280	60.83
210	60.08	290	61.02
215	60.07	300	61.28

out with an integration time step of 1 fs and the trajectories were stored every 400 fs for subsequent analyses. The minimum image convention<sup>49</sup> was employed to calculate the short-range Lennard-Jones interactions using a spherical cutoff distance of 12 Å with a switch distance of 10 Å. The long-range electrostatic interactions were calculated using the particle–mesh Ewald (PME) method.<sup>50</sup> The results reported in this work are based on the last 20 ns of each of the NPT runs. The calculations of the correlation functions along each of the trajectories have been carried out by averaging over different blocks each with 2 ns duration and separated by 200 ps from each other.

## 3. RESULTS AND DISCUSSION

**3.1. Dynamical Transition of the ss-DNA.** We have calculated several quantities from the simulated trajectories to probe the existence of “glass-like” dynamic transition for the ss-DNA molecule. First, the structural deviations of the DNA strand with respect to its minimized initial configuration have been measured by calculating the root-mean-square deviations (RMSD) between them at different temperatures. The calculations are carried out by including the non-hydrogen heavy atoms of the DNA and the time-averaged RMSD values

are shown in Figure 1a. The effect of temperature on the flexibility of the DNA strand is further probed by calculating

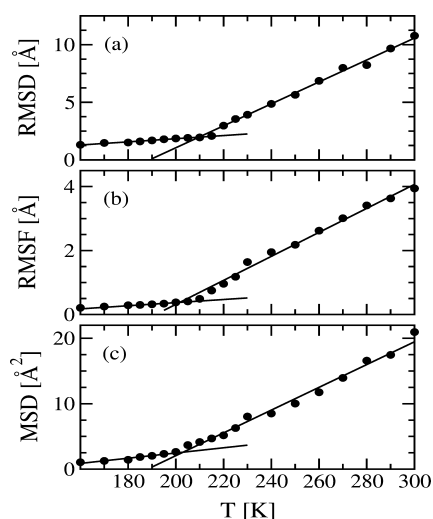


**Figure 1.** (a) Time-averaged root-mean-square deviations (RMSD) of the DNA oligomer with respect to its initial configuration, (b) the corresponding root-mean-square fluctuations (RMSF) with respect to the time-averaged configurations of the oligomer, and (c) the cumulative average mean square displacements (MSD) of the non-hydrogen DNA atoms over 100 ps durations at different temperatures.

the time-averaged root-mean-square fluctuations (RMSF) of the simulated DNA configurations with respect to the corresponding average structure at each of the temperatures. The results are shown in Figure 1b. It can be seen that both the quantities start increasing linearly from the low temperature until a sudden change in the gradient indicating onset of a structural transformation of the DNA strand occurring in the temperature range of 200 to 220 K. Such dynamical crossover should affect the local motions of the DNA atoms. To explore that we have measured the mean square displacements (MSD) of the non-hydrogen atoms of the DNA strand,  $\langle \Delta r^2(t) \rangle$ , at different temperatures.  $\langle \Delta r^2(t) \rangle$  is defined as

$$\langle \Delta r^2(t) \rangle = \langle |\mathbf{r}_i(t) - \mathbf{r}_i(0)|^2 \rangle \quad (1)$$

where  $\mathbf{r}_i(t)$  and  $\mathbf{r}_i(0)$  are the  $i$ th atom position vectors of the DNA at time  $t$  and at  $t = 0$ , respectively. The calculations are carried out by averaging over all the DNA non-hydrogen atoms and over different time origins. The cumulative  $\langle \Delta r^2 \rangle$  values over a duration of 100 ps at all the temperatures are plotted in Figure 1c. The results show excellent correlation between the temperature-dependent motions of the DNA atoms and the conformational oscillations of the DNA oligomer. We find that the average MSD values increase with temperature from low values in a linear manner up to about 200 K. This is followed by a sudden change in the gradient with further increase in temperature. It indicates that the onset of dynamical transition of the DNA strand is associated with a distinct increase in motions of the constituent atoms. To obtain a qualitative estimation of the transition temperature, we have fitted each of the data sets in Figure 1 with two best straight lines. Distinct difference between the gradients of the two lines in each case is clearly visible from the figure. The DNA crossover temperatures ( $T_{\text{DNA}}$ ) as obtained from the intersection points of these lines corresponding to the RMSD, RMSF, and MSD data are found to be within 200–220 K. It can be seen that considering

the inherent flexibility of the ss-DNA molecule and limitations of the simulation length scales, the results obtained are consistent with each other. In a recent study, the transition temperature of a double-stranded DNA (ds-DNA) molecule has been reported to be 247 K.<sup>31</sup> In addition, a large number of different biomolecules are found to exhibit similar crossovers within the temperature range of 200–240 K.<sup>9,27,29</sup> Thus, the crossover temperature of the ss-DNA as obtained from our study falls within the range generally observed for biomolecules. However, interestingly, we find that the ss-DNA chain being more flexible undergoes such transition within a narrower temperature range that is on relatively lower side of the scale than that observed for ds-DNA and other macromolecules. Further studies are necessary to compare the dynamic crossovers of ss-DNAs with that of other relatively rigid biomolecules in a more quantitative manner.

**3.2. Dynamical Transition of Hydration Water.** It is generally known that the dynamic transitions exhibited by biomolecules are solvent-induced.<sup>51</sup> The transition of the ss-DNA oligomer as observed in the previous section is therefore expected to be associated with similar dynamical crossover of the surrounding water layer. We explore that in this section by probing the temperature dependence of different dynamical properties of water molecules hydrating the DNA strand. In particular, the calculations are carried out with those water molecules that are present within 5 Å from the atoms of the DNA. This essentially corresponds to the first hydration layer around the DNA. It is important to note at this stage that dynamic exchange between waters present in the hydration layer around the DNA and those in the bulk may occur during the simulations. Consequently, a water molecule after leaving the hydration layer may also re-enter at a later time along its trajectory. To take into account such dynamic exchange, all the calculations presented in this section are averaged over the durations of the trajectory of a tagged water during which it is found to reside within the first hydration layer (i.e., within 5 Å from the DNA oligomer).

**3.2.1. Translational and Rotational Motions.** The influence of the DNA structural transition on the translational motions of the first hydration layer water molecules is investigated by monitoring their mean square displacements (MSD) (eq 1). As mentioned in the previous section, the calculations are averaged over all the tagged water molecules and over different time origins. The cumulative average MSD ( $\langle \Delta r^2 \rangle$ ) values for water over 10 ps duration are plotted as a function of temperature in Figure 2a. In Figure 2b, we show the variation of the diffusion coefficients ( $D$ ) of the hydration water at different temperatures as obtained from the corresponding MSD data using Einstein's formulation.<sup>49</sup> It may be noted that waters at the surface of a complex biomolecule are known to exhibit sublinear diffusion patterns.<sup>52,53</sup> Therefore, the differences between the  $D$  values rather than their absolute values are more important in the present context in providing a relative dynamical picture of the hydration water molecules. Interestingly, a careful examination of the results indicate a two-step dynamical crossover for the water layer hydrating the DNA strand. Again, we have fitted the data with straight lines and from the intersection points estimated the two crossover temperatures of hydration water ( $T_W$ ) to be within 210–220 K and 180–185 K, respectively. Note that the first  $T_W$  observed within 210–220 K on lowering the system temperature coincides well with the  $T_{\text{DNA}}$  range as found earlier (see section 3.1). This is an important finding that suggests that the dynamical crossover of the flexible ss-DNA



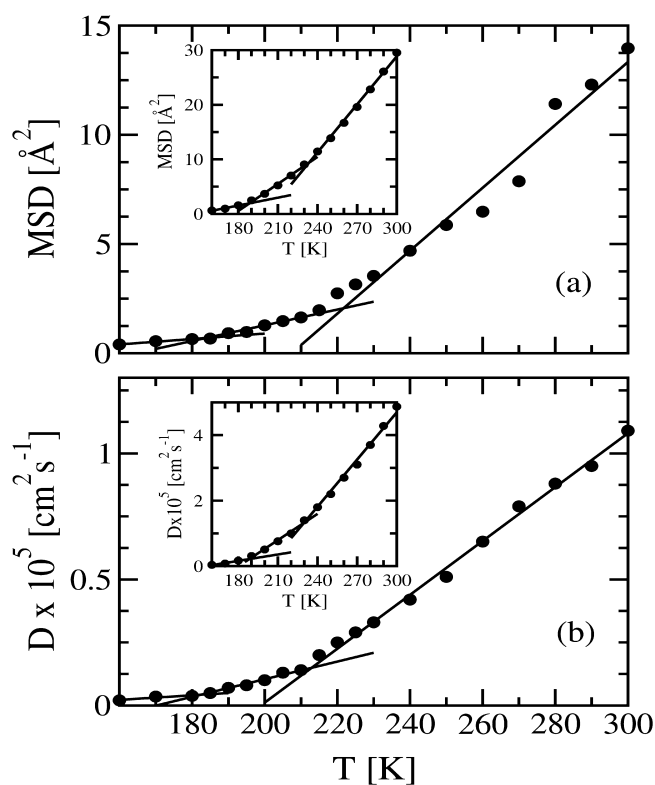


**Figure 2.** (a) Cumulative average mean square displacements (MSD) over 10 ps durations, and (b) the diffusion coefficients ( $D$ ) as obtained from the MSD data for the water molecules that are present in the first hydration layer around the DNA oligomer at different temperatures. The insets show the corresponding data for pure bulk TIP3P water.

molecule is correlated with that exhibited by its hydration water. The existence of another crossover point at a relatively lower temperature (180–185 K) is an interesting observation that qualitatively agrees with similar two-step transitions in protein hydration water detected from experimental and simulation studies.<sup>19,54</sup> Note that the temperature difference between the two crossover points as observed in our study is less compared to that reported for proteins.<sup>19</sup> We believe that this is due to the small size and high flexibility of the DNA strand as compared to proteins in aqueous media. We will discuss later the possible microscopic origin of two dynamic crossovers of the DNA hydration water. It would be interesting to compare the dynamic crossovers of the DNA hydration water with that observed for water in pure bulk state in absence of the DNA. For that, we have carried out simulations of pure TIP3P water at different temperatures. Following the same protocol as described above, we have measured the temperature-dependent mean square displacements and diffusion coefficients of bulk water, and the results are shown in the insets of Figure 2. Interestingly, the results indicate existence of two possible dynamic crossovers for TIP3P water in pure bulk state too, at around 230 and 190 K, respectively. Comparison of the results between the hydration layer water and water in bulk state reveals that the overall sluggish dynamics of water hydrating the DNA oligomer is associated with shifting of crossover points to relatively lower temperatures. However, further studies are necessary to understand the origin of such influence of the DNA.

To further understand how hydration water dynamics is coupled with that of the ss-DNA molecule during the

transition, we have calculated the translational and rotational self-intermediate scattering functions (ISF) for the first hydration layer water molecules. The translational ISF is defined as<sup>55</sup>

$$F_{tr}(k, t) = \langle \exp(-ik(\mathbf{r}_i(t) - \mathbf{r}_i(0))) \rangle \quad (2)$$

where  $k$  is the wave vector, and  $\mathbf{r}_i(t)$  and  $\mathbf{r}_i(0)$  denote oxygen atom position vectors of the  $i$ -th tagged water molecule at time  $t$  and  $t = 0$ , respectively. As mentioned earlier, the calculations are averaged over all the tagged water molecules and over different reference initial times. The value of  $|k|$  is taken to be  $1.5 \text{ \AA}^{-1}$  in the calculations. The relaxation patterns of  $F_{tr}(k, t)$  at different temperatures above and below the transition points are shown in Figure 3. Expectedly, the relaxation of the

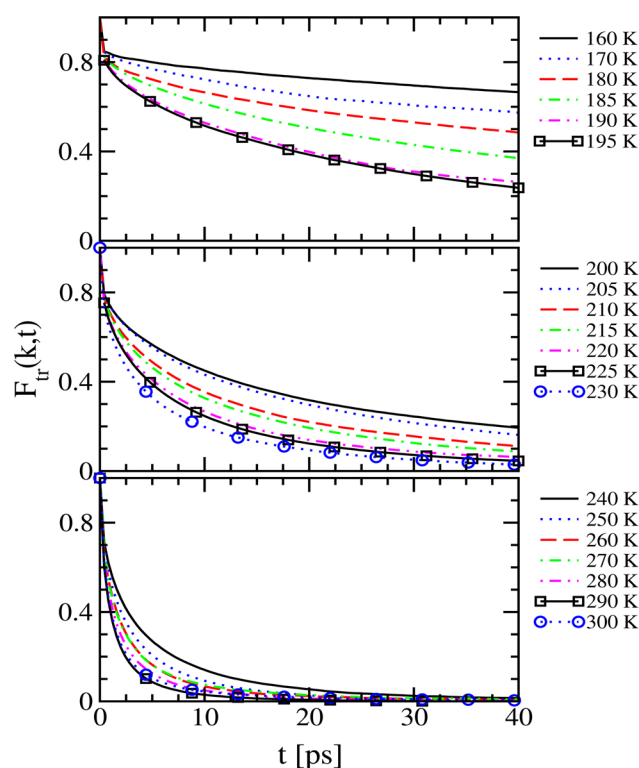


**Figure 3.** Translational intermediate scattering function (ISF),  $F_{tr}(k, t)$ , for the water molecules that are present in the first hydration layer around the DNA oligomer at different temperatures.

function slows down on lowering the temperature. However, the relative degree of slowness increases distinctly as the temperature drops below the first transition point ( $\sim 220 \text{ K}$ ). The effect is even more prominent below 190 K, as evident from the figure. This is consistent with our earlier discussion and indicates sharp increase in rigidity of the hydration layer at low temperatures. In Figure 4, we show the relaxations of the hydration water rotational ISF ( $F_{rot}(k, t)$ ), defined as

$$F_{rot}(k, t) = \langle \exp(-ik(\mathbf{d}_i(t) - \mathbf{d}_i(0))) \rangle \quad (3)$$

at different temperatures. Here,  $\mathbf{d}_i(t)$  and  $\mathbf{d}_i(0)$  are the position vectors of an hydrogen atom of the  $i$ th tagged water molecule with respect to its center of mass at time  $t$  and  $t = 0$ , respectively. As mentioned earlier, the calculations are based on averaging over the hydrogen atoms of all the tagged water molecules at different reference initial times. It is evident that along with the translational component, the relaxations of

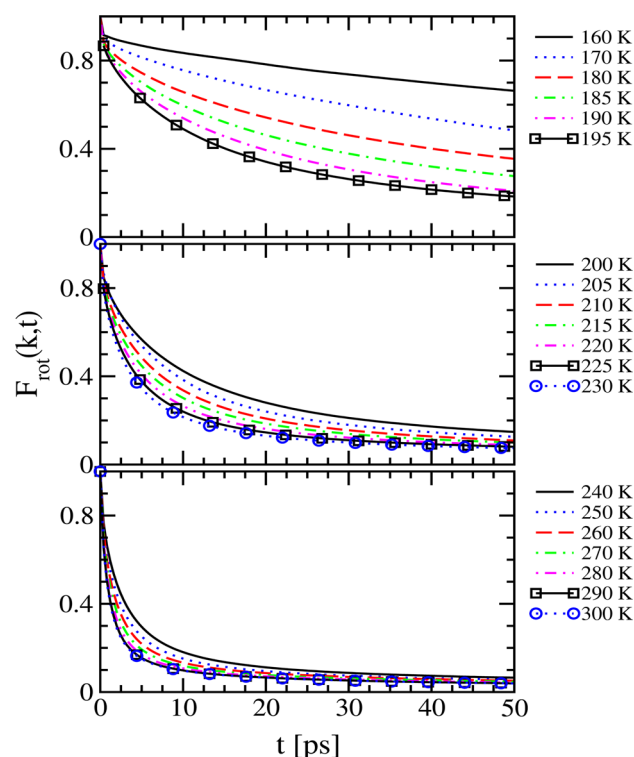


**Figure 4.** Rotational intermediate scattering function (ISF),  $F_{rot}(k,t)$ , for the water molecules that are present in the first hydration layer around the DNA oligomer at different temperatures.

rotational motions of the first hydration layer water molecules are also influenced by temperature in a similar manner. Near frozen hydration layer with drastically retarded water rotations below the crossover points is clearly visible from the data.

We have estimated the translational and rotational relaxation times of hydration waters at different temperatures by fitting the decay curves in Figures 3 and 4 with triexponentials<sup>56,57</sup> of the form

$$F(k, t) = \sum_{i=1}^3 A_i(k) \exp(-t(k)/\tau_i(k)) \quad (4)$$

where  $\tau_i(k)$  and  $A_i(k)$  correspond to different time constants and their amplitudes, respectively. The amplitude-weighted average translational and rotational relaxation times ( $\langle\tau_{tr}(k)\rangle$  and  $\langle\tau_{rot}(k)\rangle$ ) as obtained from such fits at different temperatures are shown in Figure 5, parts a and b, respectively. It is clear that on reducing the temperature from 300 K, both  $\langle\tau_{tr}(k)\rangle$  and  $\langle\tau_{rot}(k)\rangle$  values increase gradually up to about 220 K. On reducing the temperature further, distinct two-step crossovers of hydration water relaxations have been observed with sharp increase of the corresponding relaxation times. From linear fits of the data we obtain the two crossover temperatures ( $T_W$ ) for the hydration water translational relaxations to be around 213 and 188 K, while that for the rotational relaxations are around 220 and 190 K, respectively. We find that the  $T_W$  values obtained from these calculations are in the same range as that calculated earlier from water diffusion coefficients (Figure 2). Further, sharp jumps in the gradients for the data shown in Figure 5 below the crossover points indicate near frozen “glass-like” hydration layer under such conditions. By fitting the translational relaxation time data below 220 K with Arrhenius behavior  $\langle\tau_{tr}(k)\rangle = \tau_0 \exp(E_a/RT)$ , we have obtained an

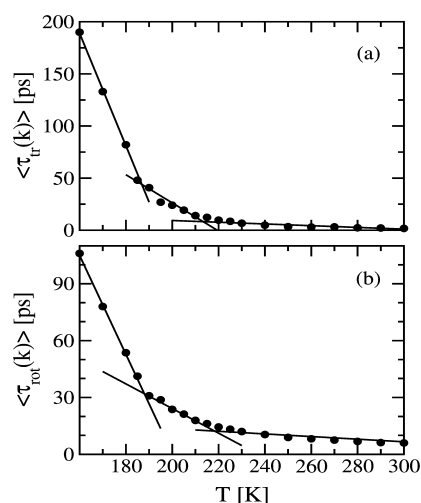


**Figure 5.** Average (a) translational and (b) rotational relaxation times ( $\langle\tau_{tr}(k)\rangle$  and  $\langle\tau_{rot}(k)\rangle$ ) for the water molecules that are present in the first hydration layer around the DNA oligomer at different temperatures.

estimate of the activation energy ( $E_a$ ) for such glassy hydration waters to be around 1 kcal mol<sup>−1</sup>. Chen et al<sup>29</sup> in a recent quasi-elastic neutron scattering (QENS) study on ds-DNA have estimated such activation energy to be around 3.5 kcal mol<sup>−1</sup>. Under the limitations of the potential model employed, our calculations demonstrate that high degree of flexibility of the single DNA strand significantly reduces the activation barrier for the dynamic crossover of its hydration water as compared to a rigid ds-DNA.

**3.2.2. Hydrogen Bond Network Analysis.** It is clear from the discussion so far that the water molecules present around the DNA strand exhibit two distinct dynamic crossovers, as evident from the diffusion coefficient data and the measured translational and rotational relaxation times. The first crossover point observed at around 210–220 K has been found to be coupled with the transition detected for the ss-DNA. The second crossover point for the hydration water observed at a relatively lower temperature in the range 180–190 K is found to be associated with the onset of near-frozen “glass-like” rigid dynamics of water. It is known that the presence of a biomolecule in aqueous environment perturbs the regular water–water hydrogen bond network at the interface due to formation of relatively stronger hydrogen bonds between the biomolecule and water.<sup>58</sup> The time scales associated with the breaking and formation of such biomolecule–water hydrogen bonds are shown to be correlated with the dynamics of water molecules hydrating the biomolecular surface.<sup>59,60</sup> Therefore, one can expect that the dynamic crossovers exhibited by the hydration water molecules as discussed in the previous section should originate from the hydrogen bond rearrangements around the DNA strand. We explore that in this section by probing the DNA–water (DW) and water–water (WW) hydrogen bond relaxations at the interface.

DNA molecule can act as a donor or an acceptor during the formation of a hydrogen bond with water. Therefore, it is first necessary to define appropriate criteria to probe different types of hydrogen bonds. Following the definitions used in our earlier work,<sup>59</sup> we have employed criteria based on specific geometrical arrangements of the participating atoms to define DW and WW hydrogen bonds in the present work. In this approach, the first condition for an atom of DNA to form a hydrogen bond with

water is that the distance between the participating DNA atom and the oxygen atom of the tagged water be within 3.3 Å. The second condition for a DNA acceptor atom (X) to form a DW hydrogen bond is that the angle between one of the O–H bond vectors of the water and the vector connecting the water oxygen atom and X be within 35°. Similarly, for a DNA donor atom (Y) to form such bond, the angle between Y–H bond vector and the vector connecting Y and the water oxygen atom should be within 35°. In addition, two water molecules are considered to be hydrogen bonded if their interoxygen and nonbonded oxygen–hydrogen distances are less than 3.5 and 2.45 Å, respectively, and the oxygen–oxygen–hydrogen angle is less than 30°. The relaxations of DW and WW hydrogen bonds are then studied by calculating the intermittent hydrogen bond time correlation function (TCF),  $C(t)$ , defined as<sup>64,65</sup>

$$C(t) = \frac{\langle h(0)h(t) \rangle}{\langle h(0)h(0) \rangle} \quad (5)$$

where,  $h(t)$  is a hydrogen bond population variable that is either 1 or 0. If a pair of sites are hydrogen bonded at a particular time  $t$ , then  $h(t) = 1$ , otherwise it is 0. The angular brackets indicate that the results reported are based on averaging over all the hydrogen bonds of a particular type that are formed at different reference initial times. According to the definition,  $C(t)$  is the probability of finding a hydrogen bond intact at time  $t$  after it was formed at  $t = 0$ . Therefore,  $C(t)$  takes into account breaking and reformation of hydrogen bonds in the intermediate times and also the long-time diffusive behavior.

Relaxations of the function  $C_{DW}(t)$  for the DW hydrogen bonds at different temperatures are shown in Figure 6. The

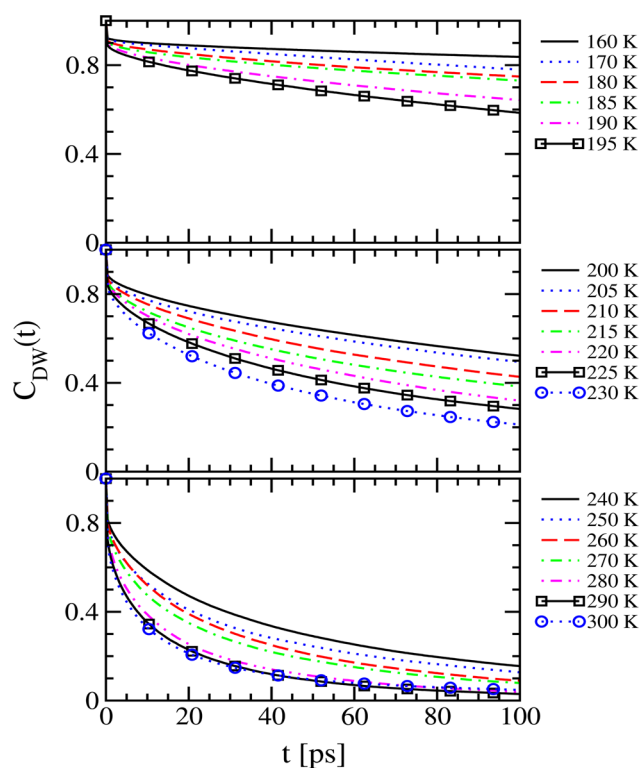


**Figure 6.** Intermittent hydrogen bond time correlation function,  $C_{DW}(t)$ , for the DW hydrogen bonds formed between the DNA oligomer and the water molecules around it at different temperatures.

calculations of the function  $C_{WW}(t)$  for the WW hydrogen bonds involving the first hydration layer water molecules around the DNA strand have also been carried out and the results are displayed in Figure 7. In agreement with the

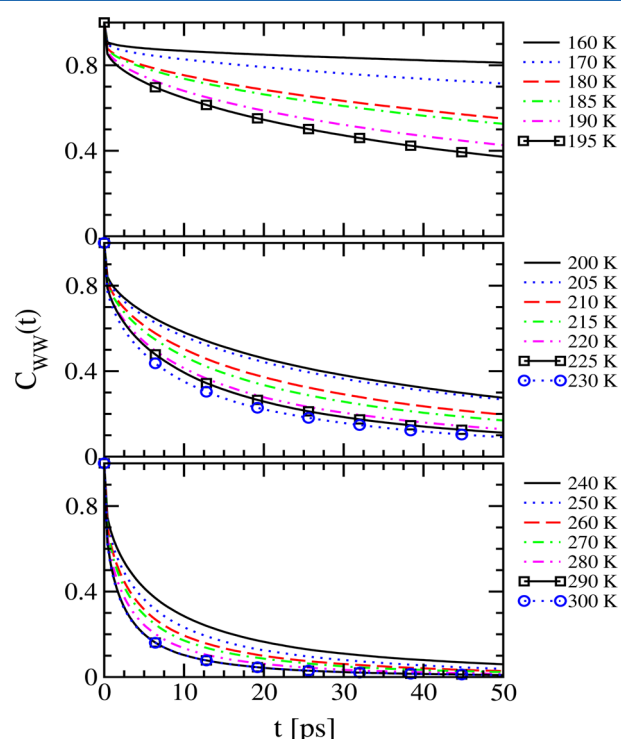


**Figure 7.** Intermittent hydrogen bond time correlation function,  $C_{WW}(t)$ , for the WW hydrogen bonds formed by the water molecules present in the first hydration layer around the DNA oligomer at different temperatures.

dynamical response of hydration water as discussed earlier, relaxations of both  $C_{DW}(t)$  and  $C_{WW}(t)$  slow down on lowering the temperature. Such correlations indicate that irrespective of the temperature the relaxation time scales of DW and WW hydrogen bonds around the DNA directly influence the mobility of the interfacial water molecules. The average relaxation times of DW and WW hydrogen bonds ( $\langle \tau_C^{DW} \rangle$  and  $\langle \tau_C^{WW} \rangle$ ) at different temperatures as obtained from triexponential fittings of the decay curves (eq 4) are shown in Figure 8, parts a and b, respectively. Note that at any given temperature the DW hydrogen bonds take significantly longer time to relax as compared to the WW hydrogen bonds. This is consistent with earlier studies of biomolecular systems<sup>60</sup> and indicates highly rigid arrangement of the water molecules that are anchored with the charged and/or polar groups of the DNA strand at the surface. Importantly, it can be seen that the degree of slowness in the relaxation patterns of  $C_{DW}(t)$  and  $C_{WW}(t)$  increases significantly near and below the dynamic crossover points. This is particularly evident from distinct two-step jumps in average relaxation times as shown in Figure 8. These are important observations that indicate modifications in hydrogen bond network environment around the DNA strand at the crossover points, thereby leading to sudden discontinuities in the time scales of formation and breaking of hydrogen bonds. Note that the temperatures around which the two crossovers in the relaxation times of DW and WW hydrogen bonds at the interface occur coincide well with the crossover temperatures

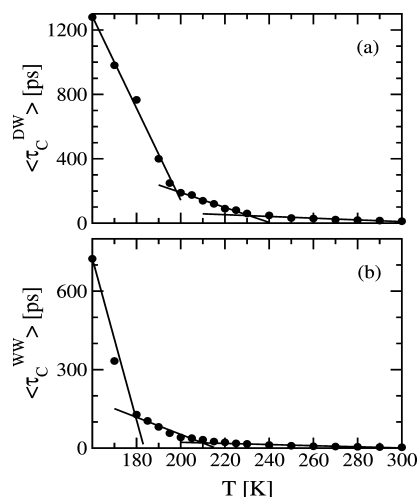


**Figure 8.** Average (a) DW and (b) WW hydrogen bond relaxation times ( $\langle \tau_C^{DW} \rangle$  and  $\langle \tau_C^{WW} \rangle$ ) involving the water molecules present in the first hydration layer around the DNA oligomer at different temperatures.

observed for the hydration water motions, which in turn correlate well with the transition temperature exhibited by the ss-DNA oligomer, as discussed in the earlier sections. It is apparent that drastic increase of the relaxation times of the DW and WW hydrogen bonds at the interface below the crossover temperatures make the DNA oligomer structurally rigid by freezing its conformational fluctuations. This clearly demonstrates that modified hydrogen bond environment at the interface is the microscopic origin of the dynamical crossovers of the hydrated DNA oligomer.

To further analyze how the hydrogen bond network environment around the DNA strand is modified with temperature, we have calculated the fractions of water molecules ( $F_W$ ) that are present in the first hydration layer around the DNA and involved in forming 2, 3, and 4 hydrogen bonds (either WW or DW type). The results are shown in Figure 9. Existence of noticeable populations of all the three types of water molecules around room temperature (300 K) can be seen from the figure. However, with decrease in temperature the population of water molecules forming two hydrogen bonds is found to decrease steadily accompanied by a simultaneous increase in the population of water molecules forming four hydrogen bonds. On the other hand, the fraction

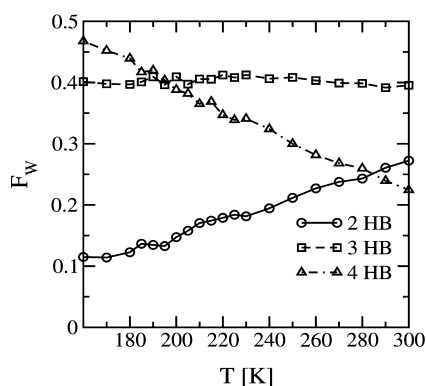


**Figure 9.** Fractions of water molecules present in the first hydration layer around the DNA oligomer that are involved in forming 2, 3, and 4 hydrogen bonds (either WW or DW type) at different temperatures.

of water molecules with three hydrogen bonds remains almost unaffected within the temperature range. The results indicate cooperative rearrangements of hydrogen bond network due to population transitions from two-coordinated to four-coordinated water molecules at the interface with lowering of temperature. Similar cooperative reordering of hydrogen bond network has been observed recently in protein hydration layer.<sup>19</sup> Interestingly, the four-coordinated water molecules are found to become the major species in the first hydration layer below the second crossover point (190 K). Such preference indicates realignment of highly frozen water molecules at the surface toward tetrahedral arrangements below 190 K.

We now attempt to quantify the effect of lowering of temperature on relative tetrahedral ordering of the surface water molecules. This is done by calculating the order parameter  $q_{tet}$ <sup>66,67</sup> defined as

$$q_{tet} = 1 - \frac{3}{8} \sum_{j=1}^3 \sum_{k=j+1}^4 \left( \cos \psi_{jk} + \frac{1}{3} \right)^2 \quad (6)$$

for the water molecules that are present around the DNA oligomer in its first hydration layer at different temperatures. Here,  $\psi_{jk}$  is the angle between the bond vectors  $\mathbf{r}_{ij}$  and  $\mathbf{r}_{ik}$ , with  $j$  and  $k$  being the four nearest neighbor atoms of the  $i$ th tagged water molecule. It is assumed in the calculations that the non-hydrogen atoms of the DNA oligomer can also act as neighboring atoms for the tagged surface water molecules. The distributions  $P(q_{tet})$  of the order parameter at different temperatures are shown in Figure 10a–c. The distributions reveal two distinct broad bands with peaks around  $q_{tet}$  of 0.5

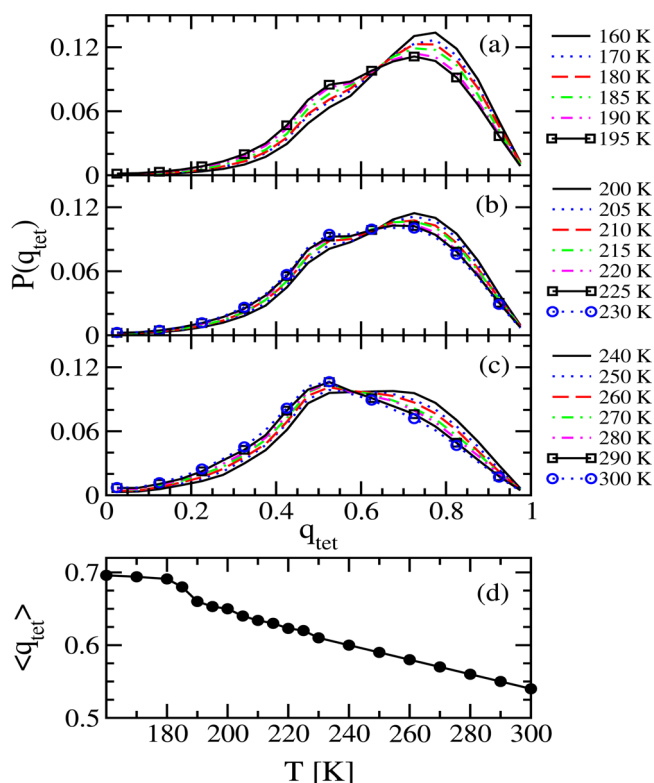


**Figure 10.** (a–c) Distributions of the tetrahedral order parameter,  $P(q_{tet})$ , and (d) the average order parameter values,  $\langle q_{tet} \rangle$ , for the water molecules that are present in the first hydration layer around the DNA oligomer at different temperatures.



and 0.75 at higher and lower temperatures, respectively. The distributions indicate steady shifts from relatively lower to higher tetrahedral ordering of the water molecules hydrating the DNA oligomer with lowering of system temperature. Such increased preference for tetrahedral arrangement of the surface water molecules with lowering of temperature is further evident from the plot of their average order parameter values ( $\langle q_{tet} \rangle$ ) with temperature as shown in Figure 10d. The increased  $\langle q_{tet} \rangle$  values on lowering the temperature also demonstrate cooperative local rearrangements of hydration waters leading to a transition from a high density liquid (HDL) like structuring at higher temperatures to that of a low density liquid (LDL) in the supercooled form at low temperatures.<sup>68</sup> Such transition from HDL to LDL with lowering of temperature has also been observed in aqueous protein solutions.<sup>51</sup> Our findings show that the  $q_{tet}$  is a parameter that can be used as a probe to monitor such structural transitions of hydration water.

#### 4. CONCLUSIONS

In this work, we have presented results obtained from about 600 ns atomistic MD simulations of a single-stranded DNA (ss-DNA) oligomer with heterogeneous distribution of nucleobases in aqueous medium at different temperatures ranging from 160 to 300 K. The correlated low temperature dynamic crossovers of the DNA strand and that of its hydration water have been explored by measuring different dynamic properties of the system. Efforts have been made to identify the microscopic origin of such correlated transitions.

The calculations reveal onset of a distinct dynamical crossover of the structure of the DNA oligomer within 200–220 K. Such structural transition of the DNA strand has been found to be associated with abrupt changes in the motions of the DNA atoms within the same temperature range. The crossover temperature of the DNA strand as obtained from our calculations has been found to be in the range as that observed for different biomolecular systems.<sup>9,27,29</sup> Interestingly, calculations of water diffusivities and the translational and rotational relaxation times reveal existence of two-step dynamical crossovers for the hydration layer water molecules within 210–220 K and 180–185 K, respectively. Importantly, the first crossover point exhibited by the hydration water within 210–220 K has been found to coincide well with the temperature range in which the DNA oligomer exhibits conformational transition. This demonstrates that the dynamical crossover of the DNA strand is correlated with that exhibited by its hydration water. Existence of the second crossover temperature for the DNA hydration water at a lower temperature (180–185 K) indicates onset of a highly frozen “glass-like” water layer around the DNA, which qualitatively agrees with similar two-step transitions observed for water hydrating other biomolecules.<sup>19,54</sup> Our calculations further demonstrate that the cooperative rearrangement of water hydrogen bond network occurring at the interface with lowering of temperature is the microscopic origin of hydration water dynamic crossovers. Importantly, it is found that such rearrangements around the crossover points occur due to population transition from two-coordinated to four-coordinated tetrahedrally ordered water molecules. This in turn indicates cooperative transition from a high density liquid (HDL)-like structuring at higher temperatures to that of a low density liquid (LDL) at low temperatures.

It is worth mentioning at this stage that the conformational behavior of a hydrated ss-DNA oligomer depends on its

nucleobase sequence as well as on the presence of additional salt. Thus, it would be interesting to probe whether the variation of base sequence and presence of salt have any influence on coupled dynamic crossovers of DNA oligomers and their hydration waters. Presently, we are exploring these issues in our laboratory.

#### AUTHOR INFORMATION

##### Corresponding Author

\*(S.B.) Telephone: +91-3222-283344. Fax: +91-3222-255303. E-mail: sanjoy@chem.iitkgp.ernet.in.

##### Notes

The authors declare no competing financial interest.

#### ACKNOWLEDGMENTS

This study was supported in part by a grant from the Department of Science and Technology (DST) (SR/S1/PC-23/2007), Government of India. Part of the work was carried out using the computational facility created under the DST-FIST programme (SR/FST/CSII-011/2005). K.C. thanks the CSIR, Government of India, for providing a scholarship.

#### REFERENCES

- (1) Nelson, D. L.; Cox, M. M. *Lehninger Principles of Biochemistry*; 3rd Ed.; Worth: New York, 2000.
- (2) Cantor, C. R.; Schimmel, P. R. *Biophysical Chemistry*; Freeman: New York, 2004.
- (3) Kumar, P.; Yan, Z.; Xu, L.; Mazza, M. G.; Buldyrev, S. V.; Chen, S. H.; Sastry, S.; Stanley, H. E. Glass Transition in Biomolecules and the Liquid-liquid Critical Point of Water. *Phys. Rev. Lett.* **2006**, *97*, 177802.
- (4) Ngai, K. L.; Capaccioli, S.; Shinyashiki, N. The Protein “Glass” Transition and the Role of the Solvent. *J. Phys. Chem. B* **2008**, *112*, 3826–3832.
- (5) Teeter, M. M.; Yamano, A.; Mohanty, U. On the Nature of a Glassy State of Matter in a Hydrated Protein: Relation to Protein Function. *Proc. Natl. Acad. Sci. U.S.A.* **2001**, *98*, 11242–11247.
- (6) Doster, W.; Cusack, S.; Petry, W. Dynamical Transition of Myoglobin Revealed by Inelastic Neutron Scattering. *Nature* **1989**, *337*, 754–756.
- (7) Parak, F.; Knapp, E. W.; Kucheida, D. Protein Dynamics: Mössbauer Spectroscopy on Deoxymyoglobin Crystals. *J. Mol. Biol.* **1982**, *161*, 177–194.
- (8) Khodadadi, S.; Pawlus, S.; Roh, J. H.; Sakai, V. G.; Mamontov, E.; Sokolov, A. P. The Origin of the Dynamic Transition in Proteins. *J. Chem. Phys.* **2008**, *128*, 195106.
- (9) Chu, X.; Zhang, Y.; Fratini, E.; Baglioni, P.; Faraone, A.; Chen, S. H. Observation of a Dynamic Crossover in RNA Hydration Water Which Triggers a Dynamic Transition in the Biopolymer. *Phys. Rev. E* **2008**, *77*, 011908.
- (10) Doster, W. The Protein-Solvent Glass Transition. *Biochim. Biophys. Acta* **2010**, *1804*, 3–14.
- (11) Schirò, G.; Caronna, C.; Natali, F.; Koza, M. M.; Cupane, A. The Protein Dynamical Transition Does Not Require the Protein Polypeptide Chain. *J. Phys. Chem. Lett.* **2011**, *2*, 2275–2279.
- (12) Mamontov, E.; Chu, X. Waterprotein Dynamic Coupling and New Opportunities for Probing it at Low to Physiological Temperatures in Aqueous Solutions. *Phys. Chem. Chem. Phys.* **2012**, *14*, 11573–11588.
- (13) Capaccioli, S.; Ngai, K. L.; Ancherbak, S.; Paciaroni, A. Evidence of Coexistence of Change of Caged Dynamics at  $T_g$  and the Dynamic Transition at  $T_d$  in Solvated Proteins. *J. Phys. Chem. B* **2012**, *116*, 1745–1757.
- (14) Schirò, G.; Natali, F.; Cupane, A. Physical Origin of Anharmonic Dynamics in Proteins: New Insights From Resolution-Dependent

Neutron Scattering on Homomeric Polypeptides. *Phys. Rev. Lett.* **2012**, 109, 128102.

(15) Tarek, M.; Tobias, D. J. Role of Protein-Water Hydrogen Bond Dynamics in the Protein Dynamical Transition. *Phys. Rev. Lett.* **2002**, 88, 138101.

(16) Hayward, J. A.; Smith, J. Temperature Dependence of Protein Dynamics: Computer Simulation Analysis of Neutron Scattering Properties. *Biophys. J.* **2002**, 82, 1216–1225.

(17) Glass, D. C.; Krishnan, M.; Nutt, D. R.; Smith, J. C. Temperature Dependence of Protein Dynamics Simulated with Three Different Water Models. *J. Chem. Theory. Comput.* **2010**, 6, 1390–1400.

(18) Matyushov, D. V. Nanosecond Stokes Shift Dynamics, Dynamical Transition, and Gigantic Reorganization Energy of Hydrated Heme Proteins. *J. Phys. Chem. B.* **2011**, 115, 10715–10724.

(19) Mazza, M. G.; Stokely, K.; Pagnotta, S. E.; Bruni, F.; Stanley, H. E.; Franzese, G. More than One Dynamic Crossover in Protein Hydration Water. *Proc. Natl. Acad. Sci. U.S.A.* **2011**, 108, 19873–19878.

(20) Mallamace, F.; Chen, S. H.; Broccio, M.; Corsaro, C.; Crupi, V.; Majolino, D.; Venuti, V.; Baglioni, P.; Fratini, E.; Vannucci, C.; Stanley, H. E. Role of the Solvent in the Dynamical Transitions of Proteins: The Case of the Lysozyme-Water System. *J. Chem. Phys.* **2007**, 127, 045104.

(21) R  t, V.; Dunn, R.; Ferrand, M.; Finney, J. L.; Daniel, R. M.; Smith, J. C. Solvent Dependence of Dynamic Transitions in Protein Solutions. *Proc. Natl. Acad. Sci. U.S.A.* **2000**, 97, 9961–9966.

(22) Roh, J. H.; Novikov, V. N.; Gregory, R. B.; Curtis, J. E.; Chowdhuri, Z.; Sokolov, A. P. Onsets of Anharmonicity in Protein Dynamics. *Phys. Rev. Lett.* **2005**, 95, 038101.

(23) Russo, D.; Gonzalez, M. A.; Pellegrini, E.; Combet, J.; Olliver, J.; Teixeira, J. Evidence of Dynamical Constraints Imposed by Water Organization Around a Bio-hydrophobic Interface. *J. Phys. Chem. B* **2013**, 117, 2829–2836.

(24) Arcangeli, C.; Bizzarri, A. R.; Cannistraro, S. Role of Interfacial Water in the Molecular Dynamics-simulated Dynamical Transition of Plastocyanin. *Chem. Phys. Lett.* **1998**, 291, 7–14.

(25) Tarek, M.; Tobias, D. J. The Dynamics of Protein Hydration Water: A Quantitative Comparison of Molecular Dynamics Simulations and Neutron-scattering Experiments. *Biophys. J.* **2000**, 79, 3244–3257.

(26) Doster, W.; Settles, M. Protein-Water Displacement Distributions. *Biochem. Biophys. Acta.* **2005**, 1749, 173–186.

(27) Curtis, J. E.; Dirama, E. T.; Carri, A. G.; Tobias, D. J. Inertial Suppression of Protein Dynamics in a Binary Glycerol/Trehalose Glass. *J. Phys. Chem. B.* **2006**, 110, 22953–22956.

(28) Zaccai, G. How Soft Is a Protein? A Protein Dynamics Force Constant Measured by Neutron Scattering. *Science* **2000**, 288, 1604–1607.

(29) Chen, S. H.; Liu, L.; Chu, X.; Zhang, Y.; Fratini, E.; Baglioni, P.; Faraone, A.; Mamontov, E. Experimental Evidence of Fragile-to-strong Dynamic Crossover in DNA Hydration Water. *J. Chem. Phys.* **2006**, 125, 171103.

(30) Fenimore, P. W.; Frauenfelder, H.; McMahon, B. H.; Parak, F. G. Slaving: Solvent Fluctuations Dominate Protein Dynamics and Functions. *Proc. Natl. Acad. Sci. U.S.A.* **2002**, 99, 16047–16051.

(31) Biswal, D.; Jana, B.; Pal, S.; Bagchi, B. Dynamical Transition of Water in the Grooves of DNA Duplex at Low Temperature. *J. Phys. Chem. B* **2009**, 113, 4394–4399.

(32) Wood, K.; Fr  lich, A.; Paciaroni, A.; Moulin, M.; H  rtlein, M.; Zaccai, G.; Tobias, D.; Weik, M. Coincidence of Dynamical Transitions in a Soluble Protein and Its Hydration Water: Direct Measurements by Neutron Scattering and MD Simulations. *J. Am. Chem. Soc.* **2008**, 130, 4586–4587.

(33) Norberg, J.; Nilsson, L. Glass Transition in DNA from Molecular Dynamics Simulations. *Proc. Natl. Acad. Sci. U.S.A.* **1996**, 93, 10173–10176.

(34) Kumar, P.; Yan, Z.; Xu, L.; Mazza, M. G.; Buldyrev, S. V.; Chen, S. H.; Sastry, S.; Stanley, H. E. Glass Transition in Biomolecules and

the Liquid-Liquid Critical Point of Water. *Phys. Rev. Lett.* **2006**, 97, 177802.

(35) Murphy, M. C.; Rasnik, I.; Cheng, W.; Lohman, T. M.; Ha, T. Probing Single-Stranded DNA Conformational Flexibility Using Fluorescence Spectroscopy. *Biophys. J.* **2004**, 86, 2530–2537.

(36) Zou, L.; Elledge, S. J. Sensing DNA Damage Through ATRIP Recognition of RPA-ssDNA Complexes. *Science* **2003**, 300, 1542–1548.

(37) Chakraborty, K.; Mantha, S.; Bandyopadhyay, S. Molecular Dynamics Simulation of a Single-stranded DNA with Heterogeneous Distribution of Nucleobases in Aqueous Medium. *J. Chem. Phys.* **2013**, 139, 075103.

(38) Cui, S.; Albrecht, C.; K  hner, F.; Gaub, H. E. Weakly Bound Water Molecules Shorten Single-Stranded DNA. *J. Am. Chem. Soc.* **2006**, 128, 6636–6639.

(39) Miyamoto, K.; Onodera, K.; Yamaguchi, R.; Ishibashi, K.; Kimura, Y.; Niwano, M. Hydration of Single-stranded DNA in Water Studied by Infrared Spectroscopy. *Chem. Phys. Lett.* **2007**, 436, 233–238.

(40) Kaji, T.; Ito, S.; Iwai, S.; Miyasaka, H. Nanosecond to Submillisecond Dynamics in Dye-labeled Single-stranded DNA, As Revealed by Ensemble Measurements and Photon Statistics at Single-molecule Level. *J. Phys. Chem. B* **2009**, 113, 13917–13925.

(41) Buhot, A.; Halperin, A. Effects of Stacking on the Configurations and Elasticity of Single-stranded Nucleic Acids. *Phys. Rev. E.* **2004**, 70, 020902.

(42) Sen, S.; Nilsson, L. MD Simulations of Homomorphous PNA, DNA, and RNA Single Strands: Characterization and Comparison of Conformations and Dynamics. *J. Am. Chem. Soc.* **2001**, 123, 7414–7422.

(43) Philips, J. C.; Braun, R.; Wang, W.; Gumbart, J.; Tajkhorshid, E.; Villa, E.; Chipot, C.; Skeel, R. D.; Kale, L.; Schulten, K. Scalable Molecular Dynamics with NAMD. *J. Comput. Chem.* **2005**, 26, 1781–1802.

(44) Foloppe, N.; MacKerell, A. D., Jr. All-Atom Empirical Force Field for Nucleic Acids: I. Parameter Optimization Based on Small Molecule and Condensed Phase Macromolecular Target Data. *J. Comput. Chem.* **2000**, 21, 86–104.

(45) MacKerell, A. D., Jr.; Banavali, N. All-Atom Empirical Force Field for Nucleic Acids: II. Application to Molecular Dynamics Simulations of DNA and RNA in Solution. *J. Comput. Chem.* **2000**, 21, 105–120.

(46) Jorgensen, W. L.; Chandrasekhar, J.; Madura, J. D.; Impey, R. W.; Klein, M. L. Comparison of Simple Potential Functions for Simulating Liquid Water. *J. Chem. Phys.* **1983**, 79, 926–935.

(47) Tereshko, V.; Minasov, G.; Egli, M. The Dickerson-Drew B-DNA Dodecamer Revisited at Atomic Resolution. *J. Am. Chem. Soc.* **1999**, 121, 470–471.

(48) Feller, S. E.; Zhang, Y.; Pastor, R. W.; Brooks, B. R. Constant Pressure Molecular Dynamics Simulation: The Langevin Piston Method. *J. Chem. Phys.* **1995**, 103, 4613–4621.

(49) Allen, M. P.; Tildesley, D. J. *Computer Simulation of Liquids*; Clarendon: Oxford, U.K., 1987.

(50) Darden, T.; York, D.; Pedersen, L. Particle Mesh Ewald: An  $N \log(N)$  Method for Ewald Sums in Large Systems. *J. Chem. Phys.* **1993**, 98, 10089–10092.

(51) Chen, S. H.; Liu, L.; Fratini, E.; Baglioni, P.; Faraone, A.; Mamontov, E. Observation of Fragile-to-strong Dynamic Crossover in Protein Hydration Water. *Proc. Natl. Acad. Sci. U.S.A.* **2006**, 103, 9012–9016.

(52) Rocchi, C.; Bizzarri, A. R.; Cannistraro, S. Water Dynamical Anomalies Evidenced by Molecular-Dynamics Simulations at the Solvent-Protein Interface. *Phys. Rev. E* **1998**, 57, 3315–3325.

(53) Pizzitutti, F.; Marchi, M.; Sterpone, F.; Rossky, P. J. How Protein Surfaces Induce Anomalous Dynamics of Hydration Water. *J. Phys. Chem. B* **2007**, 111, 7584–7590.

(54) Zanolli, J. M.; Gibrat, G.; Bellissent-Funel, M. C. Hydration Water Rotational Motion as a Source of Configurational Entropy

Driving Protein Dynamics. Crossovers at 150 and 220 K. *Phys. Chem. Chem. Phys.* **2008**, *10*, 4865–4870.

(55) Chen, S. H.; Gallo, P.; Sciortino, F.; Tartaglia, P. Molecular-dynamics Study of Incoherent Quasielastic Neutron-scattering Spectra of Supercooled Water. *Phys. Rev. E* **1997**, *56*, 4231.

(56) Cola, D. D.; Deriu, A.; Sampoli, M.; Torcini, A. Density Functional Theory of Crystal Growth: Lennard Jones Fluids. *J. Chem. Phys.* **1996**, *104*, 4223–4232.

(57) Sayeed, A.; Mitra, S.; Kumar, A. V. A.; Mukhopadhyay, R.; Yashonath, S.; Chaplot, S. L. Diffusion of Propane in Zeolite NaY: A Molecular Dynamics and Quasi-Elastic Neutron Scattering Study. *J. Phys. Chem. B* **2003**, *107*, 527–533.

(58) Bizzarri, A. R.; Cannistraro, S. Molecular Dynamics of Water at the Protein Solvent Interface. *J. Phys. Chem. B* **2002**, *106*, 6617–6633.

(59) Sinha, S. K.; Bandyopadhyay, S. Local Heterogeneous Dynamics of Water Around Lysozyme: A Computer Simulation Study. *Phys. Chem. Chem. Phys.* **2012**, *14*, 899–913.

(60) Pal, S.; Bandyopadhyay, S. Importance of Protein Conformational Motions and Electrostatic Anchoring Sites on the Dynamics and Hydrogen Bond Properties of Hydration Water. *Langmuir* **2013**, *29*, 1162–1173.

(61) Luzar, A.; Chandler, D. Structure and Hydrogen Bond Dynamics of Water-Dimethyl Sulfoxide Mixtures by Computer Simulations. *J. Chem. Phys.* **1993**, *98*, 8160–8173.

(62) Luzar, A.; Chandler, D. Hydrogen-Bond Kinetics in Liquid Water. *Nature* **1996**, *379*, 55–57.

(63) Luzar, A.; Chandler, D. Effect of Environment on Hydrogen Bond Dynamics in Liquid Water. *Phys. Rev. Lett.* **1996**, *76*, 928–931.

(64) Stillinger, F. H. Water Revisited. *Science* **1980**, *209*, 451–457.

(65) Rapaport, D. C. Hydrogen Bonds in Water Network Organization and Lifetimes. *Mol. Phys.* **1983**, *50*, 1151–1162.

(66) Chau, P. L.; Hardwick, A. J. A New Order Parameter for Tetrahedral Configurations. *J. Mol. Phys.* **1998**, *93*, 511–518.

(67) Errington, J. R.; Debenedetti, P. G. Relationship Between Structural Order and the Anomalies of Liquid Water. *Nature* **2001**, *409*, 318–321.

(68) Xu, L.; Mallamace, F.; Yan, Z.; Starr, F. W.; Buldyrev, S. V.; Stanley, H. E. Appearance of a Fractional Stokes-Einstein Relation in Water and a Structural Interpretation of Its Onset. *Nature Phys.* **2009**, *5*, 565–569.